

Mechanism-Guided Engineering of ω -Transaminase to Accelerate Reductive Amination of Ketones

Sang-Woo Han,^{+,a} Eul-Soo Park,^{+,a} Joo-Young Dong,^a and Jong-Shik Shin^{a,*}

^a Department of Biotechnology, Yonsei University, Shinchon-Dong 134, Seodaemun-Gu, Seoul 120-749, South Korea
Fax: (+82)-2-362-7265; phone: (+82)-2-2123-5884; e-mail: enzymo@yonsei.ac.kr

⁺ These authors contributed equally to this work.

Received: March 1, 2015; Published online: May 13, 2015



Supporting information for this article is available on the WWW under <http://dx.doi.org/10.1002/adsc.201500211>.

Abstract: Asymmetric reductive amination of ketones using ω -transaminases (ω -TAs) offers a promising alternative to the chemocatalytic synthesis of chiral amines. One fundamental challenge to the biocatalytic strategy is the very low enzyme activities for most ketones compared with native substrates (i.e., <1% relative to pyruvate). Here we have demonstrated that a single point mutation in the active site of the (*S*)-selective ω -TA from *Ochrobactrum anthropi* could induce a remarkable acceleration of the amination reaction without any loss in stereoselectivity and enzyme stability. Molecular modeling of quinonoid intermediates, alanine scanning mutagenesis and kinetic analysis revealed that the W58 residue

acted as a steric barrier to binding and catalytic turnover of ketone substrates. Removal of the steric strain by W58L substitution, which was selected by partial saturation mutagenesis, led to dramatic activity improvements for structurally diverse ketones (e.g., 340-fold increase in k_{cat}/K_M for acetophenone). The W58L mutant afforded an efficient synthesis of enantiopure amines (i.e., >99% *ee*) using isopropylamine as an amino donor.

Keywords: asymmetric amination; chiral amines; molecular modeling; protein engineering; ω -transaminases

Introduction

Asymmetric synthesis of chiral compounds *via* biocatalytic strategies has attracted growing attention as an alternative to chemocatalytic methods due to environmental and social demands for green processes in the chemical industry.^[1] To harness the full capacity of biocatalysts as synthetic toolkits, enzyme properties such as stability, substrate range and optimal reaction conditions should be compatible with a manufacturing setting.^[2] However, the design of a biocatalytic process is often limited by sophisticated enzyme properties evolved for biological fitness that is incongruous with industrial demands.^[3] A typical example is ω -transaminase (ω -TA) which possesses a unique catalytic capability affording the stereoselective transfer of an amino group from primary amines to carbonyl compounds without an external cofactor such as NADH.^[4] Spurred by the versatile utility of chiral amines as essential building blocks for a number of pharmaceuticals and fine chemicals,^[5] there has been a massive research effort to synthesize enantiopure

amines from prochiral ketones using ω -TAs.^[6] Inconsistent with the industrial need, ω -TAs have not evolved to exploit ketones as native amino acceptors but rather a limited range of keto acids (i.e., pyruvate and glyoxylate)^[7] as observed with other types of transaminases.^[8] This biologically driven substrate bias leads to very low activities of all known ω -TAs for most ketones (i.e., <1% relative to pyruvate). For example, the (*S*)-selective ω -TA from *Ochrobactrum anthropi* (OATA) exhibits only 0.03% activity for acetophenone (i.e., a typical ketone substrate) relative to pyruvate (see Table S1 in the Supporting Information). Such a low substrate reactivity should be compensated by high enzyme dosage to achieve reasonable reaction rates, which poses a significant challenge for implementing a scalable process.

In addition to the poor kinetic performance for ketones, asymmetric synthesis of chiral amines using ω -TAs has suffered from an unfavorable reaction equilibrium.^[6a] Recent studies to cope with the thermodynamic limitation have proved that an equilibrium shift can be efficiently driven by several reaction engineer-

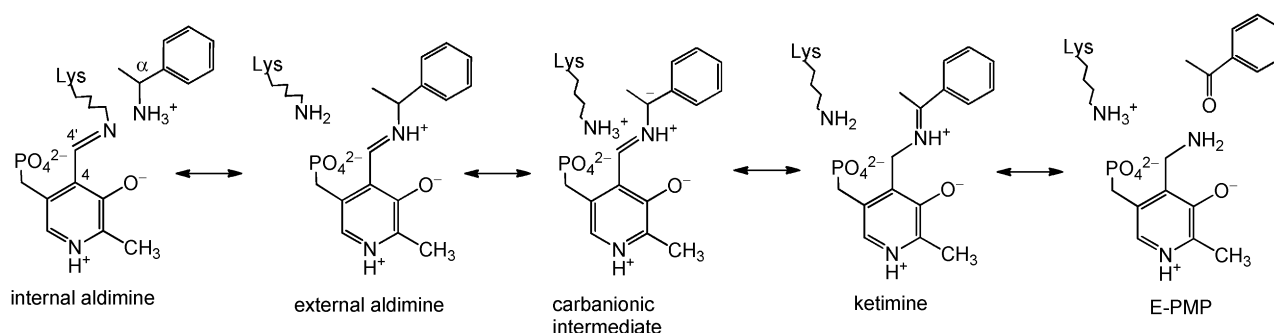
ing strategies employing enzymatic or physicochemical removal of a co-product.^[9] However, only a few examples of tackling the kinetic limitation are available.^[6d,10] To boost the synthetic utility of ω -TAs, it is imperative to develop a facile strategy for the creation of enzyme variants displaying desirable kinetic properties with ketones. In this regard, Savile et al. demonstrated an expansion of substrate specificity of (*R*)-selective ω -TA from *Arthrobacter* sp. (ARTA) by protein engineering involving 27 amino acid substitutions.^[6d] Contrary to expectations, the engineered variant of ARTA showed a modest activity improvement toward acetophenone (i.e., only 46% increase; Supporting Information, Table S2). Moreover, the massive mutations led to a significant loss in the stereoselectivity toward some ketones (e.g. benzylacetone; Supporting Information, Table S3). This led us to explore the feasibility of whether active site redesign involving minimal mutations could fulfill a desirable improvement in amination kinetics for structurally diverse ketones without deteriorating essential parental properties such as stereoselectivity. To this end, OATA was chosen for protein engineering owing to its exceptionally high activity for isopropylamine^[11] which is an ideal amino donor for industrial applications.^[6d] Instead of time-consuming iterative library generation and selection, we sought to pinpoint a key residue by mechanism-based structural modeling and optimize the hot spot by saturation mutagenesis.

Results and Discussion

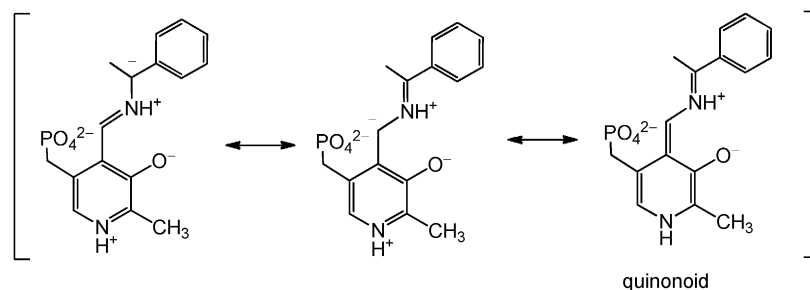
Structural Modeling of Quinonoid Intermediates

ω -TA exploits pyridoxal 5'-phosphate (PLP) as a prosthetic group to mediate the transfer of an amino group.^[4] The whole reaction consists of two half reactions (i.e., oxidative deamination of an amino donor and reductive amination of an amino acceptor), which involves multiple reaction intermediates (Scheme 1).^[12] The PLP form of the enzyme is present as a Schiff base formed with an active site lysine (i.e., internal aldimine). Transaldimination with an incoming amino donor converts the internal aldimine to an external aldimine (i.e., a Schiff base between PLP and the amino donor). Abstraction of a C- α hydrogen from the external aldimine produces an unstable carbanionic intermediate that is converted to a ketimine after protonation at the C-4' position. Hydrolysis of the ketimine leads to the formation of a ketone product and a pyridoxamine 5'-phosphate (PMP) form of the enzyme (i.e., E-PMP). The reverse reaction (i.e., from E-PMP to the internal aldimine) represents the reductive amination of acetophenone.

It is generally accepted that the carbanionic intermediate is the most unstable reaction intermediate which should be resonance-stabilized by a quinonoid form (Scheme 2).^[13] Thus, effective stabilization of the quinonoid in the active site is known to be pivotal in the transaminase reactions.^[13] This led us to posit that



Scheme 1. Detailed reaction pathway showing the oxidative deamination of α -methylbenzylamine.



Scheme 2. Resonance structures of the carbanionic intermediate.

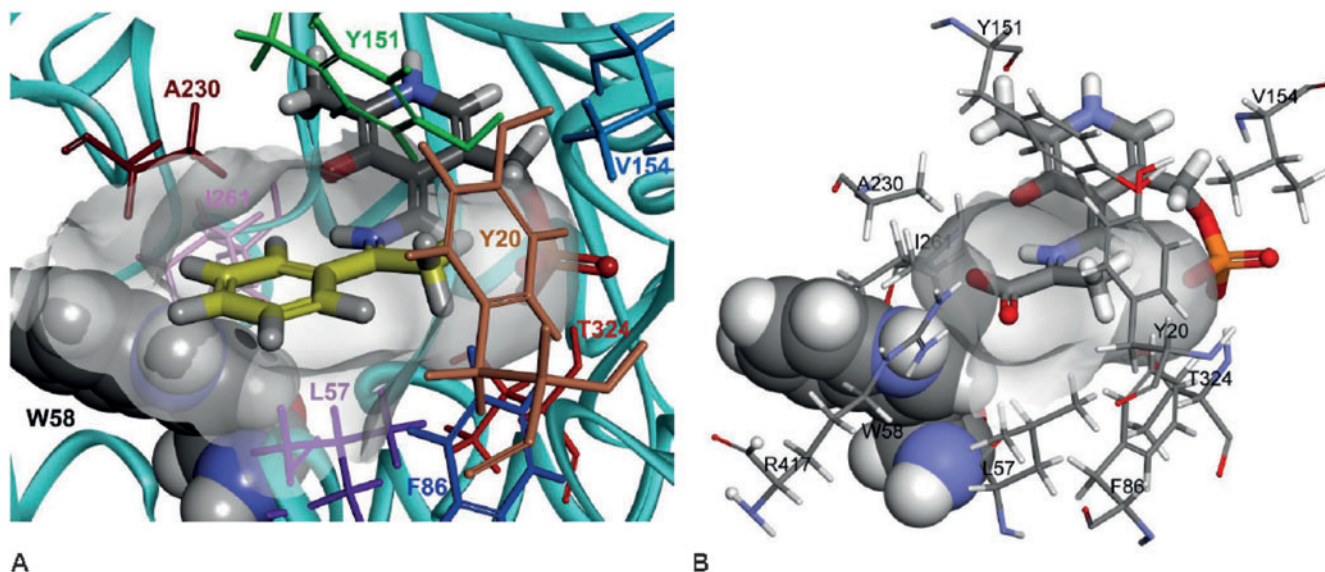


Figure 1. Molecular model of the quinonoid intermediates in the active site of OATA. Thick sticks represent the quinonoid intermediate. Thin sticks represent nine active site residues (i.e., Y20, L57, W58, F86, Y151, V154, A230, I261 and T324). W58 is shown in a CPK representation. **A)** Acetophenone-quinonoid intermediate where the substrate moiety is colored in yellow. Color use of the active site residues is consistent with that of labels. **B)** Pyruvate-quinonoid intermediate. R417 is a conserved active site residue that forms hydrogen bonds with a carboxylate of the keto acid substrate. The active site arginine is known to undergo a gross conformational change, depending on the hydrophobic type of the incoming substrate.^[14]

the very low activity of ω -TAs toward ketones, relative to native amino acceptors, would result from a failure in the effective stabilization of the quinonoid intermediate. Therefore, we performed *in silico* modeling of the two quinonoids formed with acetophenone and pyruvate to compare differences in the structural environments. The molecular model identified six active site residues (i.e., L57, W58, Y151, A230, I261 and T324) whose side chains lay within a 3 Å distance from the substrate moiety of the quinonoid formed with acetophenone (Figure 1A). Among the nearby residues, W58 was found to engender a severe steric interference with the phenyl substituent of acetophenone. In contrast, no steric interference of the quinonoid formed with pyruvate was observed against the proximal active site residues (Figure 1B). The modeling results suggest that the steric strain caused by W58 destabilizes the quinonoid intermediate formed with a bulky ketone and thereby leads to the drastic reduction in the reactivity of ketones.

Alanine Scanning Mutagenesis

Structural models of the two quinonoid intermediates predict that substitution of W58 with a smaller residue would relieve the steric strain and consequently induce an activity enhancement for acetophenone. To test this notion, we performed alanine scanning mutagenesis of active site residues, shown in Figure 1

except for A230, and assessed whether the model prediction was in accordance with experimental results (Table 1). Indeed, W58A mutation led to an abrupt activity improvement for acetophenone (i.e., 41-fold increase) and the substitution with alanine elsewhere did not elicit such an activity increase except for modest activity improvements by V154A and I261A. To visualize whether the W58A mutation relieved the steric strain, we performed molecular modeling of the acetophenone-quinonoid in the W58A mutant (Supporting Informationb, Figure S1). The model prediction supported that the activity improvement came

Table 1. Effect of alanine scanning mutagenesis of active site residues on the amination of acetophenone.^[a]

Mutation	Reaction rate ^[b] ($\times 10^{-2} \mu\text{M min}^{-1}$)	Fold increase
none	8.26 \pm 0.90	–
Y20A	3.52 \pm 0.25	0.4
L57A	4.78 \pm 0.41	0.6
W58A	340 \pm 37	41
F86A	n.d. ^[c]	\approx 0
Y151A	0.12 \pm 0.01	0.01
V154A	13.6 \pm 0.1	1.7
I261A	23.1 \pm 0.1	2.9
T324A	3.93 \pm 0.06	0.5

^[a] Reaction conditions: 10 mM acetophenone and 10 mM L-alanine in phosphate buffer (50 mM, pH 7) at 37°C.

^[b] Reaction rate represents the initial rate per 1 μM enzyme.

^[c] n.d.: not detectable.

from removal of the steric strain observed with the wild-type enzyme.

Partial Saturation Mutagenesis of W58

Taken together with the modeling results, the alanine scanning mutagenesis indicated that W58 imposed a steric penalty on the quinonoid bearing a bulky substituent in the ketone moiety. Fine-tuning of the hot spot was performed on the basis of structural considerations by partial saturation mutagenesis with hydrophobic residues smaller than tryptophan (i.e., W58MVIL). Molecular modeling predicted that these substitutions allowed a reduction in the steric strain on the acetophenone-quinonoid as observed with the W58A substitution (Supporting Information, Figure S2). Hydrophilic residues were not taken into account for the substitution because W58 forms a hydrophobic patch with neighboring residues (i.e., M54, L57, V233, I261 and I380; Supporting Information, Figure S3). Enzyme activities of the resulting mutants, including W58A, were compared with those of the wild-type enzyme in the reaction with acetophenone and L-alanine as well as in its reverse reaction with (*S*)- α -methylbenzylamine [(*S*)- α -MBA] and pyruvate (Figure 2). We found a positive correlation between the enzyme activities measured with the two substrate pairs (Pearson correlation coefficient = 0.86), indicating that the mutations benefit both reactions presumably because the two reactions follow the same reaction pathway but run in the opposite direction. It is notable that all the mutations lead to much higher-fold increases in the amination of acetophenone than those in the deamination of (*S*)- α -MBA. This result indicates that the mutations accelerate the amination

of acetophenone more selectively than its reverse reaction. Considering the increases in both reaction rates, we chose the W58L mutant (OATA_{W58L}) for further study.

Activity Improvements for Various Ketones

To assess the synthetic utility of OATA_{W58L}, we examined whether the W58L substitution improved the enzyme activity toward structurally diverse ketones using isopropylamine (**2**) as an amino donor (Table 2). OATA_{W58L} showed dramatic activity improvements toward all the ketones tested [i.e., nine aryl alkyl ketones (**1a–i**) and six alkyl ketones (**1j–o**)] with 41- to 760-fold increases in the reaction rates. The activity improvements were high enough to bring about substantial reactivities of ketones that were inert with the wild-type enzyme (i.e., **1c**, **1g** and **1h**). In contrast to the engineered ARTA, OATA_{W58L} did not show any loss in stereoselectivity for the amination of all the ketones listed in Table 2 [i.e., *ee* values of the produced (*S*)-**3a–o** >99%], including benzylacetone (**1f**). It is notable that the W58L mutation affords efficient amination of bulky ketones carrying even a naphthyl (**1i**) and an *n*-hexyl (**1l**) group.

Kinetic Analysis of the W58L Mutant

To provide a mechanistic understanding on how the W58L mutation altered the catalytic properties, we carried out a kinetic analysis using four typical substrates (Table 3). OATA_{W58L} showed a 55.7-fold increase in the turnover number (i.e., k_{cat}) for **1a**, which is consistent with the modeling results (i.e., reduction in the steric strain on the quinonoid as shown in the Supporting Information, Figure S2). Moreover, the mutation promoted the formation of a Michaelis complex (i.e., 6.1-fold tighter binding), seemingly because binding of **1a** to the active site would be facilitated by the W58L mutation. Indeed, docking simulation suggested that steric interference between W58 and the phenyl substituent of **1a** was found to be severe in the Michaelis complex (Supporting Information, Figure S4). The facilitated binding in concert with the accelerated turnover led to a 340-fold increase in the specificity constant (i.e., $k_{\text{cat}}/K_{\text{M}}$) of OATA_{W58L} for **1a**. It is remarkable that k_{cat} of OATA_{W58L} for **1a** corresponds to 20% of that of OATA for pyruvate.

In contrast to **1a**, the W58L mutation resulted in much weaker binding to pyruvate (i.e., 17.5-fold increase in K_{M}). This result is ascribable to the loss of a potential hydrogen bond donor, that is, the indole group of W58, capable of interacting with the carboxylate of pyruvate (Figure 1B). Proximity of W58 to the carboxylate of pyruvate suggests that W58, in ad-

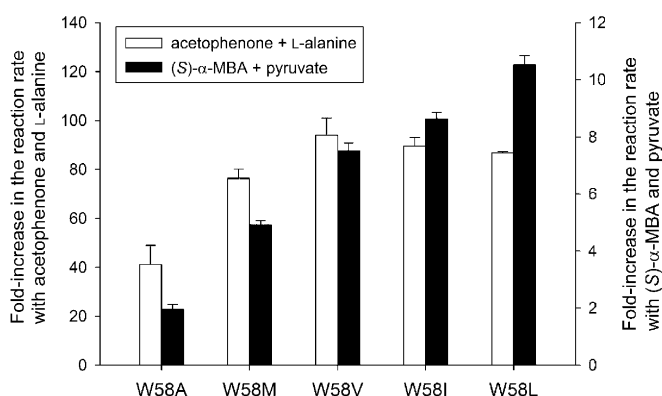


Figure 2. Partial saturation mutagenesis of the W58 residue. Fold increases represent the initial reaction rates of the mutants normalized by those of the wild-type enzyme (i.e., $8.26 \times 10^{-2} \pm 0.90 \times 10^{-2}$ and $118 \pm 2 \mu\text{M min}^{-1}$ per $1 \mu\text{M}$ enzyme for substrate pairs of acetophenone:L-alanine and (*S*)- α -MBA:pyruvate, respectively).

Table 2. Activity improvements of OATA_{W58L} toward various ketones.

Reaction scheme: Ketone (1a-o) + Isopropylamine (2) → Amino ketone (3a-o) + Pyruvate

Ketones	Substituents R ¹	R ²	Reaction rate ^[a] (μMh ⁻¹)		Fold increase
			OATA	OATA _{W58L}	
1a	-C ₆ H ₅	-CH ₃	1.92 ± 0.02	316 ± 10	165
1b	-C ₆ H ₅	-CH ₂ CH ₃	0.02 ± 0.01	5.2 ± 0.2	260
1c	-C ₆ H ₅	-(CH ₂) ₂ CH ₃	n.d. ^[b]	0.13 ± 0.01	> 130
1d	-C ₆ H ₄ - <i>p</i> -CH ₃	-CH ₃	0.97 ± 0.02	162 ± 8	167
1e	-C ₆ H ₄ - <i>p</i> -OCH ₃	-CH ₃	0.55 ± 0.01	110 ± 2	200
1f	-(CH ₂) ₂ C ₆ H ₅	-CH ₃	10.3 ± 0.1	885 ± 5	86
1g			n.d. ^[b]	7.6 ± 0.1	> 760
1h			n.d. ^[b]	2.1 ± 0.1	> 210
1i	-1-naphthyl	-CH ₃	0.82 ± 0.02	150 ± 10	183
1j	-(CH ₂) ₂ CH ₃	-CH ₃	1.6 ± 0.1	445 ± 15	278
1k	-(CH ₂) ₃ CH ₃	-CH ₃	2.9 ± 0.1	895 ± 40	309
1l	-(CH ₂) ₅ CH ₃	-CH ₃	4.0 ± 0.2	670 ± 30	167
1m	-CH(CH ₃) ₂	-CH ₃	3.1 ± 0.1	250 ± 55	81
1n	-CH ₂ CH(CH ₃) ₂	-CH ₃	0.40 ± 0.01	195 ± 5	487
1o	-cyclopropyl	-CH ₃	0.32 ± 0.01	13.0 ± 0.1	41

^[a] Reaction rates represent initial rates per 1 μM enzyme. *Reaction conditions:* 10 mM ketone and 10 mM isopropylamine in phosphate buffer (50 mM, pH 7) containing 15% v/v DMSO at 37 °C.

^[b] n.d.: not detectable. Considering the detection limit, the reaction rate was less than 0.01 μMh⁻¹.

Table 3. Kinetic parameters toward typical substrates.^[a]

Substrate	Rate constants ^[b] (OATA, OATA _{W58L})			Fold increase in $k_{\text{cat}}/K_{\text{M}}$
	K_{M} [mM]	k_{cat} [$\times 10^{-3} \text{ s}^{-1}$]	$k_{\text{cat}}/K_{\text{M}}$ [$\text{M}^{-1} \text{ s}^{-1}$]	
1a	110 ± 4	18 ± 1	9.7 ± 0.4	340
pyruvate	0.12 ± 0.01	2.1 ± 0.04	2600 ± 70	0.41
(<i>S</i>)- 3a	150 ± 16	0.73 ± 0.09	24000 ± 2000	170
2	470 ± 10	53 ± 2	9700 ± 300	8.6

^[a] Kinetic parameters represent the apparent rate constants determined at a fixed concentration of cosubstrate.

^[b] Rate constants are mean values determined from three independent experiments.

dition to R417, plays a role as a hydrogen bond donor. Nevertheless, OATA_{W58L} performed a faster catalytic turnover of pyruvate than OATA did (i.e., 7.1-fold increase in k_{cat}). Taken together with the increase in k_{cat} for **1a**, this result suggests that the W58L mutation affords acceleration of the catalytic turnover irrespective of the hydrophobic nature of amino acceptors. Despite the accelerated turnover, the drastic decrease in the binding affinity led to 60% reduction in $k_{\text{cat}}/K_{\text{M}}$ for pyruvate by the W58L mutation.

The facilitated binding of OATA_{W58L} to the bulky substrate (i.e., **1a**) was even more reinforced for (*S*)-**3a** (i.e., 207-fold decrease in K_{M}). Interestingly,

OATA_{W58L} exhibited tighter binding to **2** (i.e., 8.9-fold decrease in K_{M}), implying that even a methyl substituent of an amino donor might undergo steric interference with W58. The k_{cat} values for both amino donors were not substantially altered in contrast to the remarkable increases in k_{cat} for amino acceptors, which indicates that the W58L mutation promotes the catalytic turnover for the amination step selectively over the deamination step as observed in Figure 2. As a result, increases in $k_{\text{cat}}/K_{\text{M}}$ for the amino donors are solely attributed to the promotion in the binding step. Taken together with the dramatic increase in $k_{\text{cat}}/K_{\text{M}}$ for **1a**, the 8.6-fold increase in $k_{\text{cat}}/K_{\text{M}}$ for **2** renders

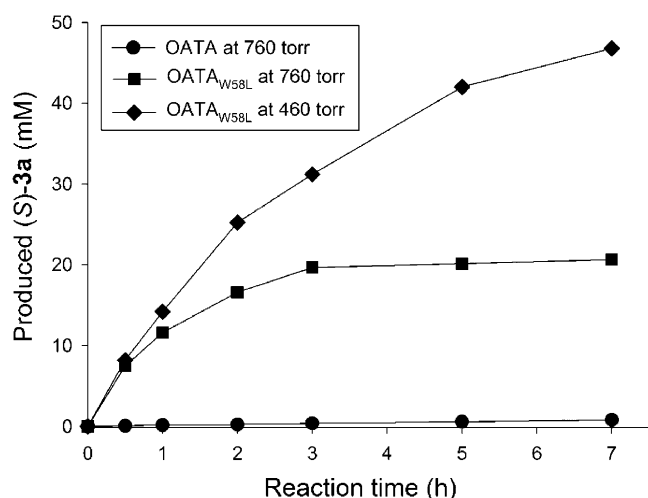


Figure 3. Asymmetric synthesis of (*S*)-**3a** using OATA_{W58L} in comparison with the wild-type enzyme. *Reaction conditions:* **1a** (50 mM), **2** (500 mM), ω -TA (5 mg mL⁻¹), PLP (0.1 mM), DMSO (15% v/v) and phosphate buffer (50 mM, pH 7.0) in a 2 mL reaction mixture.

OATA_{W58L} highly promising for scalable amination of ketones using **2** as an amino donor.

Asymmetric Synthesis of Chiral Amines

To evaluate how much the W58L mutation improved the practical utility of OATA, time-course monitoring of the asymmetric synthesis of (*S*)-**3a** from **1a** and **2** was performed at atmospheric pressure in the presence of DMSO (15% v/v) to solubilize the ketone substrate (Figure 3). As expected, OATA_{W58L} afforded a dramatic improvement in the amination of **1a** without any loss in stereoselectivity [i.e., *ee* of produced (*S*)-**3a** >99%]. No activity loss was observed for both OATA and OATA_{W58L} throughout the reaction, indicating that the W58L mutation did not affect the enzyme stability (Supporting Information, Figure S5). In contrast, the engineered ARTA showed a significant decrease in the enzyme stability compared with the wild-type ARTA under the same reaction conditions (Supporting Information, Figure S6).

Despite the high operational stability of OATA_{W58L}, the reaction progress at atmospheric pressure reached a plateau at 3 h [i.e., 39% conversion of **1a** to (*S*)-**3a**] and then further increase in the conversion was only 2% until 7 h (Figure 3). We ascribed this to an unfavorable reaction equilibrium. Based on a previous study, the equilibrium constant for the **1a**:**2** reaction in the absence of DMSO was calculated to be 5.86×10^{-2} which did not allow the concentration of produced (*S*)-**3a** to exceed 25.9 mM at the given reaction conditions.^[15] Indeed, an equilibrium shift by removing a co-product (i.e., acetone) at the reduced pres-

Table 4. Asymmetric synthesis of chiral amines using OATA_{W58L} in comparison with the wild-type enzyme.

Substrate	Reaction time [h]	Conversion ^[a] [%]		Product (% <i>ee</i>) ^[b]
		OATA	OATA _{W58L}	
1d	7	7	91	(<i>S</i>)- 3d (>99)
1f	5	26	93	(<i>S</i>)- 3f (>99)
1i	15	13	75	(<i>S</i>)- 3i (>99)
1k	10	14	93	(<i>S</i>)- 3k (>99)
1l	15	30	91	(<i>S</i>)- 3l (>99)

^[a] Conversion was calculated by analyzing (*S*)-amine produced from ketone. *Reaction conditions:* same as those in Figure 3. Reactions were carried out at 300 torr vacuum.

^[b] The *ee* values represent the ones obtained with OATA_{W58L}.

sure drove the conversion to reach 94% at 7 h with >99% *ee* of (*S*)-**3a** using OATA_{W58L}. In contrast, the engineered ARTA afforded only 19% conversion at 7 h under the same reaction conditions (Supporting Information, Figure S7).

To prove the synthetic applicability of OATA_{W58L} to the preparation of diverse chiral amines, we performed asymmetric aminations of five additional ketones (Table 4). Consistent with the activity improvements shown in Table 2, OATA_{W58L} afforded much higher conversions [i.e., >90%, except for **1i**, within 15 h with >99% *ee* of the produced (*S*)-amines] than OATA did.

One of the ketones (i.e., **1f**) was subjected to a preparative-scale synthesis in a 100-mL reaction mixture composed of **1f** (1.5 g, 10 mmol), **2** (8.6 mL, 100 mmol), DMSO (15 mL) and OATA_{W58L} (5 μ mol) at 460 torr. Conversion reached 92% at 18 h with >99% *ee* of (*S*)-**3f**. Product isolation using cation-exchange column chromatography and structural characterizations of the resulting (*S*)-**3f** were performed (see the Supporting Information), leading to recovery of pure (*S*)-**3f** (1.22 g, 81.3% isolated yield, >99% *ee*).

Conclusions

The motivation of this study was conceived with the notion that the metabolic conversion of ketones to primary amines would be irrelevant to enhancing the biological fitness of microorganisms that have evolved ω -TAs. Therefore, we posited that endowing naturally occurring ω -TAs with a decent activity for ketones by redesigning the native active site would not be chemically unachievable but could have been biologically untried. Indeed, our results clearly show that the substrate bias of a native ω -TA is amenable to engineering (i.e., from keto acids to ketones) even by a single point mutation. The W58 residue of OATA, which

serves as a crucial steric barrier to the amination of ketones, was found to be well conserved among (*S*)-selective ω -TAs (Supporting Information, Table S4). Among the fourteen ω -TAs used for multiple sequence alignment, W58 was perfectly conserved in eleven ω -TAs and was replaced by tyrosine, which also could act as a hydrogen bond donor,^[16] in the other three ω -TAs. This implies that the role of W58 to the tight interaction with the carboxylate of native keto acid substrates, as observed with aromatic amino acid transaminase,^[8] is universally played among the ω -TAs.

Experimental Section

Chemicals

Butyrophenone, 4-methyl-2-pentanone, (*S*)- α -propylbenzylamine, (*R*)- α -propylbenzylamine, (*S*)-2-aminohexane, (*R*)-2-aminohexane, (*S*)-2-aminooctane, (*R*)-2-aminooctane, (*S*)-1-cyclopropylethylamine and (*R*)-1-cyclopropylethylamine were purchased from Alfa Aesar (Ward Hill, USA). Pyruvic acid was obtained from Kanto Chemical Co. (Tokyo, Japan). Isopropylamine was purchased from Junsei Chemical Co. (Tokyo, Japan). L-Alanine was purchased from Acros Organics Co. (Geel, Belgium). Dimethyl sulfoxide (DMSO) and *n*-hexane were purchased from Duksan Pure Chemicals Co. (Ansan, Korea). All other chemicals were purchased from Sigma Aldrich Co. (St. Louis, USA). Materials used for the preparation of culture media including yeast extract, tryptone and agar were purchased from Difco. (Spark, USA).

Site-Directed Mutagenesis of ω -TA

Variants of OATA carrying a single point mutation were created by a QuikChange Lightning site-directed mutagenesis kit (Agilent Technologies Co.) according to the instruction manual. Mutagenesis primers shown in the Supporting Information, Table S5 were designed using a primer design program (<http://www.agilent.com>). The template used for the mutagenesis PCR was pET28-OATA which was previously constructed.^[12] Intended mutagenesis was confirmed by DNA sequencing.

Preparation of Purified ω -TA

Overexpression of His₆-tagged ω -TAs was carried out as described elsewhere with minor modifications.^[17] To obtain OATA, ARTA and the engineered ARTA, we used expression vectors harboring the ω -TA genes that were constructed in the previous studies.^[12,15] To obtain variants of OATA, expression vectors constructed in this study were used. *Escherichia coli* BL21(DE3) cells carrying the expression vectors [i.e., pET28a(+)] harboring the ω -TA gene were cultivated in LB medium (typically 1 L) containing 50 $\mu\text{g mL}^{-1}$ kanamycin at 37°C. IPTG was added to the culture broth (final concentration = 0.1 mM) around 0.4 OD₆₀₀ to induce protein expression and the cells were allowed to grow for 10 h. The culture broth was centrifuged (10,000 $\times g$, 10 min,

4°C) and the resulting cell pellet was resuspended in 15 mL resuspension buffer (50 mM Tris-HCl, pH 7, 50 mM NaCl, 1 mM EDTA, 1 mM β -mercaptoethanol, 0.1 mM PMSF and 0.5 mM PLP). The cell suspension was then subjected to ultrasonic disruption and centrifuged (13,000 $\times g$, 60 min, 4°C) to remove cell debris.

Protein purification was carried out on ÄKTAprime plus (GE Healthcare, Piscataway, USA). The cell-free extract was loaded on an HisTrap HP column (GE Healthcare) and the His₆-tagged ω -TA was eluted by an elution buffer (20 mM sodium phosphate, 0.5 M sodium chloride, 0.5 mM PLP, pH 7.4) with a linear gradient of imidazole (0.05–0.5 M). Removal of imidazole was carried out by a HiTrap desalting column (GE Healthcare) using an elution buffer (50 mM sodium phosphate, 0.15 M sodium chloride and 0.5 mM PLP, pH 7). When necessary, the enzyme solution was concentrated using an ultrafiltration kit (Ultracel-30) purchased from Millipore Co. (Billerica, USA).

Molar concentrations of the purified ω -TAs were determined by measuring UV absorbance at 280 nm (UV-1650PC, Shimadzu Co., Japan). Molar extinction coefficients of the homodimeric ω -TAs were obtained by protein extinction coefficient calculator (<http://www.biomol.net/en/tools/proteinextinction.htm>) and were used for concentration determination (78,076 M⁻¹ cm⁻¹ for the wild-type OATA and its variant carrying a single point mutation of L57A, F86A, V154A, I261A or T324A substitution; 67,076 M⁻¹ cm⁻¹ for OATA variants carrying a single point mutation of W58A, W58M, W58V, W58I or W58L substitution; 75,095 M⁻¹ cm⁻¹ for OATA variants carrying a single point mutation of Y20A or Y151A substitution; 101,885 M⁻¹ cm⁻¹ for ARTA; 102,135 M⁻¹ cm⁻¹ for the engineered ARTA).

Measurement of Enzyme Activity

All enzyme assays were carried out at 37°C and pH 7 (50 mM phosphate buffer). Standard substrate conditions for activity assay were 10 mM (*S*)-**3a** and 10 mM pyruvate. Typical reaction volume was 50 μL and the enzyme reaction was stopped after 30 min by adding 10 μL HCl solution (5 N). Acetophenone produced from the reactions was analyzed by HPLC. For initial rate measurements, reaction conversions were limited less than 10%.

In the reactions using acetophenone:L-alanine and (*S*)-**3a**:pyruvate substrate pairs to compare activities of OATA W58AMVIL, initial rate measurements were carried out by HPLC analysis of produced (*S*)-**3a** and acetophenone, respectively. All the substrate concentrations used in both reactions were 10 mM. The initial rate measurements were carried out separately three times.

To determine activities of OATA and OATA_{W58L} toward various ketones, a reaction mixture containing 10 mM ketone, 10 mM isopropylamine, 15% v/v DMSO and 50 mM phosphate buffer (pH 7) was used. To determine initial rates from three independent measurements, produced amines were analyzed by chiral HPLC after derivatization using Marfey's reagent.

Molecular Modeling

Molecular modeling was performed with the Discovery Studio package (version 3.5.0, Accelrys, USA) using the CHARMM force field. A homology model of OATA was

constructed using the Modeler module (version 9.8). X-ray structures of the four (*S*)-selective ω -TAs from *Paracoccus denitrificans* (PDB ID: 4GRX),^[18] *Chromobacterium violaceum* (4A6T),^[19] *Mesorhizobium loti* (3GJU)^[20] and *Rhodobacter sphaeroides* (3IST)^[20] were used as templates. The four ω -TAs assume a homodimeric structure where both active-site arginines form inward conformations (i.e., pointing away from the solvent side), except for 4GRX where one subunit harbors an outward-pointing active-site arginine. The outward-pointing arginine of 4GRX was set to be conserved in the homology model, leading to a dimeric structure of OATA where each subunit has a different conformation of the active-site arginine (i.e., an inward-pointing arginine in one subunit and an outward-pointing arginine in the other subunit). To construct a holoenzyme structure, the PLP moiety was copied from 4A6T. Sequence alignment for the homology modeling was carried out using BLOSUM62 as a scoring matrix with a default setting (−900 gap open penalty; −50 gap extension penalty). Ramachandran phi-psi analysis showed that only 0.4% non-glycine residues lay in the disallowed region, indicative of the validity of the homology model.

Active site models of OATA variants were constructed by amino acid substitution on the homology model of the wild-type OATA, followed by energy minimization (2,000 steps; dielectric constant = 4) of the mutation site as well as the proximal residues within 3 Å from W58 (i.e., M54, S55, L57, S59, G229, V233, I261, R266, I380 and C426) until the RMS gradient reached 0.1 kcal mol^{−1} Å.

Docking simulations were accomplished using the CDOCKER module under a default setting (2,000 steps at 700 K for a heating step; 5,000 steps at 300 K for a cooling step; 8 Å grid extension) within the active site defined by the Binding-Site module. The active site used for the docking simulation with L-alanine or (*S*)-**3a** was the one placed in the subunit harboring the inward- or outward-pointing arginine, respectively. The most stable docking pose showing a spatial orientation of the substrate capable of subsequent catalytic conversion was chosen and then was subjected to stepwise chemical modifications to generate an external aldimine and a quinonoid structure, each modification followed by energy minimization of K287, PLP and the substrate moiety (2,000 steps; dielectric constant = 4).

Kinetic Analysis

To obtain apparent kinetic parameters, a pseudo-one-substrate kinetic model was used under the fixed concentration of the cosubstrate.^[21] Initial rate data were fitted to a Michaelis–Menten equation, and the K_M and k_{cat} values were calculated from the slopes and y intercepts of the double-reciprocal plots. Rate constants were determined from three independent initial rate measurements over the concentration ranges of substrate and cosubstrate listed in the Supporting Information, Table S6. HPLC analytes used in the initial rate measurements are also presented in Table S6.

Small-Scale Asymmetric Synthesis of Chiral Amines

The reaction volume for the small-scale asymmetric synthesis was 2 mL and the reaction mixture was incubated at 37°C. Reaction conditions were 50 mM ketone, 500 mM **2**, 0.1 mM PLP and 5 mg mL^{−1} purified ω -TA in 50 mM phos-

phate buffer (pH 7) containing 15% v/v DMSO. For an equilibrium shift by removing acetone, the reaction mixture was incubated at 300 torr vacuum. Aliquots of the reaction mixture (50 μ L) were taken at predetermined reaction times and mixed with 10 μ L HCl solution (5N) to stop the reaction. The reaction mixtures were subjected to HPLC analysis for measurement of conversion and enantiomeric excess.

Preparative-Scale Synthesis and Isolation of (*S*)-**3f**

Preparative-scale synthesis of (*S*)-**3f** was carried out at 37°C under magnetic stirring in a round-bottom flask charged with 100 mL reaction mixture containing **1f** (1.5 g, 10 mmol), **2** (8.6 mL, 100 mmol), PLP (2.7 mg), DMSO (15 mL), OATA_{W58L} (5 μ mol) and potassium phosphate (50 mM, pH 7.0). The reaction mixture was incubated at 300 torr vacuum with a condenser running at 15°C. When the conversion of (*S*)-**3f** reached 92%, the reaction mixture was subjected to product isolation.

The pH of the reaction mixture was adjusted to 1.0 by adding 5N HCl for protein precipitation and then the resulting solution was filtered through a glass-fritted filter funnel to remove the protein precipitate. The filtrate solution was loaded on a glass column packed with Dowex 50WX8 cation-exchange resin (40 g), followed by washing with water (200 mL), and then elution was done with 150 mL of 10% ammonia solution. The elution fractions were extracted with *n*-hexane (3 \times 300 mL). The organic extractants were pooled and evaporated at 50°C and 0.25 bar.

HPLC Analysis

All the HPLC analyses were performed on a Waters HPLC system (Milford, USA). Analysis of acetophenone was performed using a Sunfire C18 column (Waters Co.) with isocratic elution of 60% methanol/40% water/0.1% trifluoroacetic acid at 1 mL min^{−1}. UV detection was done at 254 nm. Retention time of acetophenone was 3.8 min. Quantitative chiral analyses of alanine and amines were carried out using a Crownpak CR(−) column (Daicel Co., Japan) or a Sunfire C18 column after chiral derivatization with Marfey's reagent.^[22] Details of the HPLC analysis are described in the Supporting Information.

Structural Characterization of (*S*)-**3f**

The purified (*S*)-**3f** was structurally characterized by ¹H NMR, ¹³C NMR, IR and LC/MS. ¹H NMR and ¹³C NMR spectra were recorded on an Avance II FT-NMR spectrometer (Bruker Co.) using tetramethylsilane as a standard. IR spectrum was obtained by a Vertex70 FTIR spectrometer (Bruker Co.). Mass spectral data were obtained with a LTQ Orbitrap Mass Spectrometer (electrospray ionization, positive ion mode, Thermo Fisher Scientific Inc.). Details of the structural data are provided in the Supporting Information.

Acknowledgements

We acknowledge financial support from the Advanced Biomass R&D Center (ABC-2011-0031358) through the Nation-

al Research Foundation of Korea funded by the Ministry of Education, Science and Technology.

References

- [1] a) A. Schmid, J. S. Dordick, B. Hauer, A. Kiener, M. Wubbolts, B. Witholt, *Nature* **2001**, *409*, 258–268; b) S. Wenda, S. Illner, A. Mell, U. Kragl, *Green Chem.* **2011**, *13*, 3007–3047; c) C. A. Denard, J. F. Hartwig, H. Zhao, *ACS Catal.* **2013**, *3*, 2856–2864; d) B. M. Nestl, S. C. Hammer, B. A. Nebel, B. Hauer, *Angew. Chem.* **2014**, *126*, 3132–3158; *Angew. Chem. Int. Ed.* **2014**, *53*, 3070–3095.
- [2] P. Tufvesson, J. Lima-Ramos, J. S. Jensen, N. Al-Haque, W. Neto, J. M. Woodley, *Biotechnol. Bioeng.* **2011**, *108*, 1479–1493.
- [3] a) M. T. Reetz, *Angew. Chem.* **2011**, *123*, 144–182; *Angew. Chem. Int. Ed.* **2011**, *50*, 138–174; b) U. T. Bornscheuer, G. W. Huisman, R. J. Kazlauskas, S. Lutz, J. C. Moore, K. Robins, *Nature* **2012**, *485*, 185–194; c) N. J. Turner, *Nat. Chem. Biol.* **2009**, *5*, 567–573.
- [4] a) M. S. Malik, E. S. Park, J. S. Shin, *Appl. Microbiol. Biotechnol.* **2012**, *94*, 1163–1171; b) R. C. Simon, N. Richter, E. Busto, W. Kroutil, *ACS Catal.* **2013**, *4*, 129–143; c) M. Höhne, S. Schätzle, H. Jochens, K. Robins, U. T. Bornscheuer, *Nat. Chem. Biol.* **2010**, *6*, 807–813.
- [5] a) T. C. Nugent, *Chiral Amine Synthesis: Methods, Developments and Applications*, Wiley-VCH, Weinheim, **2010**; b) M. Breuer, K. Ditrich, T. Habicher, B. Hauer, M. Kessler, R. Sturmer, T. Zelinski, *Angew. Chem.* **2004**, *116*, 806–843; *Angew. Chem. Int. Ed.* **2004**, *43*, 788–824; c) D. Ghislieri, N. J. Turner, *Top. Catal.* **2014**, *57*, 284–300.
- [6] a) D. Koszelewski, K. Tauber, K. Faber, W. Kroutil, *Trends Biotechnol.* **2010**, *28*, 324–332; b) M. Höhne, U. T. Bornscheuer, *ChemCatChem* **2009**, *1*, 42–51; c) D. Koszelewski, I. Lavandera, D. Clay, G. M. Guebitz, D. Rozzell, W. Kroutil, *Angew. Chem.* **2008**, *120*, 9477–9480; *Angew. Chem. Int. Ed.* **2008**, *47*, 9337–9340; d) C. K. Savile, J. M. Janey, E. C. Mundorff, J. C. Moore, S. Tam, W. R. Jarvis, J. C. Colbeck, A. Krebber, F. J. Fleitz, J. Brands, P. N. Devine, G. W. Huisman, G. J. Hughes, *Science* **2010**, *329*, 305–309.
- [7] a) J. S. Shin, B. G. Kim, *J. Org. Chem.* **2002**, *67*, 2848–2853; b) U. Kaulmann, K. Smithies, M. E. B. Smith, H. C. Hailes, J. M. Ward, *Enzyme Microb. Technol.* **2007**, *41*, 628–637.
- [8] K. Hirotsu, M. Goto, A. Okamoto, I. Miyahara, *Chem. Rec.* **2005**, *5*, 160–172.
- [9] a) F. G. Mutti, C. S. Fuchs, D. Pressnitz, J. H. Sattler, W. Kroutil, *Adv. Synth. Catal.* **2011**, *353*, 3227–3233; b) M. Höhne, S. Kühn, K. Robins, U. T. Bornscheuer, *Chem-BioChem* **2008**, *9*, 363–365; c) S. Schätzle, F. Steffen-Munsberg, A. Thontowi, M. Höhne, K. Robins, U. T. Bornscheuer, *Adv. Synth. Catal.* **2011**, *353*, 2439–2445; d) J. S. Shin, B. G. Kim, *Biotechnol. Bioeng.* **1999**, *65*, 206–211; e) M. D. Truppo, J. D. Rozzell, N. J. Turner, *Org. Process Res. Dev.* **2010**, *14*, 234–237; f) P. Tufvesson, J. S. Jensen, W. Kroutil, J. M. Woodley, *Biotechnol. Bioeng.* **2012**, *109*, 2159–2162; g) K. E. Cassimjee, C. Branneby, V. Abedi, A. Wells, P. Berglund, *Chem. Commun.* **2010**, *46*, 5569–5571; h) A. P. Green, N. J. Turner, E. O'Reilly, *Angew. Chem. Int. Ed.* **2014**, *53*, 10714–10717.
- [10] a) K. S. Midelfort, R. Kumar, S. Han, M. J. Karmilowicz, K. McConnell, D. K. Gehlhaar, A. Mistry, J. S. Chang, M. Anderson, A. Villalobos, J. Minshull, S. Govindarajan, J. W. Wong, *Protein Eng. Des. Sel.* **2013**, *26*, 25–33; b) K. E. Cassimjee, M. S. Humble, H. Land, V. Abedi, P. Berglund, *Org. Biomol. Chem.* **2012**, *10*, 5466–5470.
- [11] E. S. Park, J. Y. Dong, J. S. Shin, *Org. Biomol. Chem.* **2013**, *11*, 6929–6933.
- [12] E. S. Park, M. Kim, J. S. Shin, *Appl. Microbiol. Biotechnol.* **2012**, *93*, 2425–2435.
- [13] a) M. D. Toney, *Arch. Biochem. Biophys.* **2014**, *544*, 119–127; b) A. C. Eliot, J. F. Kirsch, *Annu. Rev. Biochem.* **2004**, *73*, 383–415.
- [14] V. N. Malashkevich, J. J. Onuffer, J. F. Kirsch, J. N. Janssonius, *Nat. Struct. Biol.* **1995**, *2*, 548–553.
- [15] E.-S. Park, M. S. Malik, J.-Y. Dong, J.-S. Shin, *Chem-CatChem* **2013**, *5*, 1734–1738.
- [16] K. Okada, K. Hirotsu, H. Hayashi, H. Kagamiyama, *Biochemistry* **2001**, *40*, 7453–7463.
- [17] E. S. Park, J. S. Shin, *Adv. Synth. Catal.* **2014**, *356*, 3505–3509.
- [18] C. Rausch, A. Lerchner, A. Schiefner, A. Skerra, *Proteins* **2013**, *81*, 774–787.
- [19] M. S. Humble, K. E. Cassimjee, M. Håkansson, Y. R. Kimbung, B. Walse, V. Abedi, H. J. Federsel, P. Berglund, D. T. Logan, *FEBS J.* **2012**, *279*, 779–792.
- [20] F. Steffen-Munsberg, C. Vickers, A. Thontowi, S. Schätzle, T. Tumlrirsch, M. S. Humble, H. Land, P. Berglund, U. T. Bornscheuer, M. Höhne, *ChemCatChem* **2013**, *5*, 150–153.
- [21] E. S. Park, J. S. Shin, *Appl. Environ. Microbiol.* **2013**, *79*, 4141–4144.
- [22] a) C. B'Hymer, M. Montes-Bayon, J. A. Caruso, *J. Sep. Sci.* **2003**, *26*, 7–19; b) R. Bhushan, H. Brückner, *Amino Acids* **2004**, *27*, 231–247.